The combined use of acetazolamide and *Rhodiola* in the prevention and treatment of altitude sickness

Chengzhu Cao[1,2], Huan Zhang[1,2], Yongchun Huang[2], Yameng Mao[2], Lan Ma[2], Shoude Zhang[3], Wei Zhang[1,2]

[1]Research Center for High-Altitude Medicine, Key Laboratory for High-Altitude Medicine, Ministry of Education, Qinghai University, Xining, China; [2]Medical College of Qinghai University, Qinghai University, Xining, China; [3]State Key Laboratory of Plateau Ecology and Agriculture, Qinghai University, Xining, China

Contributions: (I) Conception and design: C Cao, W Zhang; (II) Administrative support: S Zhang, W Zhang; (III) Provision of study materials or patients: C Cao, H Zhang; (IV) Collection and assembly of data: C Cao, Y Huang, Y Mao, L Ma; (V) Data analysis and interpretation: C Cao, S Zhang, W Zhang; (VI) Manuscript writing: All authors; (VII) Final approval of manuscript: All authors.

Correspondence to: Prof. Wei Zhang. Research Center for High-Altitude Medicine, Key Laboratory for High-Altitude Medicine, Ministry of Education, Qinghai University, 16# Kunlun Road, Xining 810001, China. Email: zw0228@qhu.edu.cn.

Background: Altitude sickness (AS), which is caused by rapid exposure to low amounts of oxygen at high elevations, poses a great threat to humans working and traveling in these conditions. Acute mountain sickness includes high-altitude pulmonary edema and high-altitude cerebral edema. Acetazolamide (AZ) is often used to treat pulmonary edema caused by hypoxia. Additionally, the medicinal plant *Rhodiola rosea L.* (*Rh*) is often used to prevent AS in the Qinghai-Tibet plateau. However, the mechanisms of action of *Rh* and AZ in the treatment of AS remain unclear. To date, no research has been conducted to determine whether their combined use has better efficacy in the treatment and prevention of AS than their separate use.

Methods: We used the method of network pharmacology to analyze the mechanisms of *Rh* and AZ in combination in the prevention and treatment of AS, and also verified our results.

Results: The hypoxia-inducible factor (HIF)-1 signaling pathway, which is related to hypoxia, and other pathways related to pulmonary hypertension, became more enriched after the combined use of the 2 drugs. Additionally, *Rh* and AZ regulated most nodes in the AS network. Further, compared to their separate use, the combined use of *Rh* and AZ further downregulated the gene expression of HIF-1α and improved hemodynamics in rats, and thus helped the body to reduce its sensitivity to hypoxic environments and pulmonary artery pressure.

Conclusions: This study provides evidence supporting the combined use of AZ and *Rh* in the treatment of AS.

Keywords: Altitude sickness (AS); acetazolamide (AZ); *Rhodiola*; high altitude

Submitted Apr 15, 2022. Accepted for publication May 13, 2022.
doi: 10.21037/atm-22-2111
View this article at: https://dx.doi.org/10.21037/atm-22-2111

Introduction

Altitude sickness (AS) refers to the negative health effect of high altitude caused by rapid exposure to low amounts of oxygen at high elevations (i.e., elevations >2,500 m); however, susceptible individuals can also get sick at low altitudes (1). The partial pressure of oxygen is lower at high altitudes. In general, hypoxia triggers a physiological regulation that helps the body adapt to low oxygen conditions (2). Sometimes, the body responds abnormally. These abnormal reactions can include dizziness, headache, vomiting, weakness, and sleep disorders (3,4). Acute mountain sickness can progress to high-altitude pulmonary edema or high-altitude cerebral edema (5). Chronic AS may occur following long-term exposure to a high altitude (6,7).

Various treatment methods are used to treat AS-induced symptoms. These methods are mainly divided to non-pharmacological interventions and pharmacological interventions. Non-pharmacological interventions are mainly to relieve symptoms of altitude sickness by inhaling oxygen or lowering the altitude of the patient. However, this approach is often limited due to the lack of oxygen facilities or transportation in the wilderness. Currently, pharmacological interventions is often used to prevent or alleviate the symptoms of AS. Dexamethasone and acetazolamide (AZ) are the two main drugs used to treat AS-induced symptoms. Dexamethasone can block the inflammation of alveolar hypoxia at several sites in the inflammatory cascade (8). However, it has side effects of hormonal drugs and is not suitable for long-term use. AZ is a carbonic anhydrase inhibitor that is effective in preventing AS (9-12). However, its mechanism of action remains controversial. Preliminary study has shown that AZ can cause alkaluria and metabolic acidosis by inhibiting carbonic enzymes (13). This physiological change requires the body to compensate through respiratory alkalosis via hyperventilation. Ultimately, AZ improves ventilation in response to hypoxic stimuli at high altitudes (14,15). However, other study suggests that AZ causes pulmonary vasodilation and is not associated with carbonic anhydrase inhibition (16). Given such contradictory results, the mechanism of action of AZ remains unclear. Additionally, the medicinal plant *Rhodiola rosea L.* (*Rh*) is widely used to prevent or treat AS in traditional Chinese medicine (17-19). Its mechanism of action has been studied; however, it is not yet completely understood. Further, the combined use of AZ and *Rh* in the prevention and treatment of AS has not been examined.

Here, we analyzed the mechanisms of action of AZ and *Rh* in the treatment of AS both separately and in combination by the method of network of pharmacology. Network pharmacology utilizes principles of systems biology and network analysis to interpret the mechanism of drugs in a complex disease, which is aligned with the theoretical significance of the herbal formula. This method is more suitable for analyzing complex diseases, such as AS-induced symptoms. Moreover, we validated key genes and pathways from network pharmacology analysis in the rat model. Our study not only provides evidence for their combined use, but also hopefully overcomes the side effects of hormonal drugs. We present the following article in accordance with the ARRIVE reporting checklist (available at https://atm.amegroups.com/article/view/10.21037/atm-22-2111/rc).

Methods

Animals

The study was approved by the Medical Science Research Ethics Committee of Qinghai University School of Medicine (No. 2021-40), and animal handling and care procedures were conducted in accordance with institutional guidelines for the care and use of animals. All efforts were made to minimize the pain and suffering of the animals and to minimize the number of animals used. A protocol was prepared before the study without registration.

For this study, 48 Sprague-Dawley (SD) rats were purchased from Beijing Vital River Laboratory Animal Technology Co. (Beijing, China) and housed under standard light, temperature, and humidity conditions (12:12 h light/dark cycle, 21±1 ℃, 55%±5% humidity). The rats had free access to drinking water and laboratory rodent chow.

Network pharmacology analysis

Target information was collected using literature mining and reverse docking. In the mining literature, all the available target information on AZ and the chemical constituents of *Rh* was collected from the PubChem database and the Comparative Toxicogenomic Database (CTD, http://www.ctdbase.org). Only the active targets from the PubChem and interacted genes from CTD were selected from the research results. In reverse docking, PharmMapper (20,21) was used to search for possible targets for the compounds. Only the top 10 targets from all the predicted targets of each compound were selected as potential targets.

An interaction network was constructed for each protein by use of the STRING database which is an integration of known and predicted protein interactions (22). Cytoscape software (Version 3.8.4; http://www.cytoscape.org/) and the Network Analyzer plugin (Version 1.0, http://med.bioinf.mpiinf. mpg.de/netanalyzer/) were used to visualize the network and calculate the basic network parameters (23). The size of the nodes corresponds to the node degree. Other analyses were performed based on the STRING analysis modules.

RT-PCR

The healthy male SD rats (weighing 300±30 g) were randomly divided into the following four groups (n=6 rats/group): (I) the AZ group; (II) the *Rh* group; (III) the AZ + *Rh* group; and (IV) the control group. The rats in each of the

4 groups were treated with AZ [100 mg/kg, intragastrically (i.g.)], *Rh* (30 mg/kg, i.g.), AZ + *Rh* (100 mg/kg AZ and 30 mg/kg *Rh*, i.g.), and saline, respectively. The doses were selected according to previous research (24-26). All the rats were then subjected to hypoxic conditions with 15% O_2 ventilation for 0 and 5 h, respectively. Afterward, the rats were anesthetized using pentobarbitone sodium [50 mg/kg, intraperitoneal (i.p.)], and the lung tissue was removed, quickly frozen in liquid nitrogen, and ground. Total ribonucleic acid (RNA) was extracted using a TRIzol RNA kit and analyzed using reverse transcription-polymerase chain reaction (RT-PCR). The following primers were used: F5'-CCA GAT TCA AGA TCA GCC AGC A-3' and R5'-GCT GTC CAC ATC AAA GCG TAC TCA-3'.

Hemodynamics test

The experimental procedure was based on our previous methods (27). Briefly, healthy male SD rats (weighing 300±30 g) were randomly divided into the following 4 groups (n=6 rats per group): (I) the AZ group; (II) the *Rh* group; (III) the AZ + *Rh* group; and (IV) the control group. The rats in each of the 4 groups were treated with AZ (100 mg/kg, i.g.), *Rh* (30 mg/kg, i.g.), AZ + *Rh* (100 mg/kg AZ and 30 mg/kg *Rh*, i.g.), and saline for 2 h, respectively. The animals were then anesthetized using pentobarbitone sodium at a dose of 50 mg/kg. To maintain body temperature at 37±0.5 ℃, a heating pad was placed underneath each rat. The tidal volume (6–7 $mL\cdot kg^{-1}$) was adjusted according to each animal's body weight and other physiological parameters. The respiratory rate was maintained at 70 breaths per minute. To keep the lungs inflated, we maintained the positive end-expiratory pressure at 2.5 cmH_2O. We connected the intravascular cannula to the pressure transducer and then to the biosignal acquisition system of Power Lab (ML206; AD Instruments, Castle Hill, NSW, Australia) aligned to the level of the right atrium and calibrated prior to use.

Next, 4 different diameters of polyethylene catheters were inserted into the left common carotid artery, the right external jugular vein, the right ventricle, and the left atrium to measure mean arterial pressure (MAP), central venous pressure (CVP), pulmonary artery pressure (PAP), and left atrial pressure (LAP), respectively. After opening the chest cavity, a pulsed Doppler flow probe was placed under the ascending aorta to measure the ascending aortic blood flow (ABF). Mechanical ventilation was maintained via tracheal intubation and measurement airway pressure (Paw).

The experimental indicators of all groups were measured for 5 min under normoxic condition and continuously recorded for another 5 min under the hypoxic condition with 15% oxygen (O_2) ventilation. Catheters were connected to the Power Lab biological signal acquisition system for continuous real-time hemodynamic monitoring and the collation of sampling records.

Preparation of Rh extracts

The roots of *Rh* were crushed and extracted with 90% ethanol under reflux 3 times, and the ethanol was then evaporated to obtain a crude extract for subsequent experiments. A 30 mg/mL aqueous solution was used for the administration.

Data analyzing and statistical analysis

The data were analyzed using SPSS (version 27.0; SPSS, Inc., Chicago, IL, USA). The values are shown as the mean ± standard deviation. Comparisons of the means among different groups (≥3 groups) were determined using an analysis of variance. The independent sample *t*-test was used to evaluate the significance of the difference between two groups; the statistical significance was set at $P<0.05$.

Results

Network pharmacology

The ingredients of *Rh* were derived from a review, and 52 compounds were selected (28) as detailed in the supplementary material (see Figure S1). The target information about the 52 constituents of *Rh* and AZ was obtained by data mining and reverse docking. After removing any duplicates and non-Homo sapiens targets, 1400 Homo-sapiens targets were selected for the ingredients of *Rh*, and 113 Homo sapiens targets were selected for the ingredients of AZ (see Table S1).

The target-target networks of *Rh* and AZ were built by inputting the 1,400 targets of *Rh* and 113 targets of AZ into the STRING database. Additionally, an integrated network was established by importing all the targets. The topological properties of the 3 target networks are shown in *Table 1*. The degree of nodes increased after integration, indicating that many targets are shared between *Rh* and AZ. Further, after 63 nodes from the AZ-related target network were added to the *Rh*-related target network, the number

Table 1 The topological properties of the *Rh*- and AZ-related target networks

Name	*Rh*	AZ	Combined
Number of nodes	1,085	63	1,124
Number of edges	26,338	300	28,358
Average node degree	48.5	9.52	50.5
Average local clustering coefficient	0.423	0.555	0.425
Expected number of edges	14,861	89	16,263
PPI enrichment P value	$<1.0^{e-16}$	$<1.0^{e-16}$	$<1.0^{e-16}$

Rh, *Rhodiola*; AZ, acetazolamide; PPI, protein-protein interaction.

of edges increased by more than 2,000 edges, suggesting that most of the nodes in the AZ-related target network are relevant to the *Rh*-related target network. This correlation suggests that their combined use is synergistic in the treatment of certain diseases.

Herbal medicine usually exhibits diverse pharmacological activities and regulates multiple cellular pathways; thus, studying *Rh*- and AZ-related cellular pathways is helpful in analyzing the mechanism of treating AS. In this study, 210 Kyoto Encyclopedia of Genes and Genomes (KEGG) pathways were identified for *Rh*, 135 of which were found to be highly enriched (false discovery rate $<E^{-05}$) (see Table S2). Additionally, we identified 13 enriched pathways for AZ and 139 enriched pathways in the combined target network. Among these pathways, both *Rh* and AZ regulated the hypoxia-inducible factor 1 α (HIF-1α) signaling pathway, which is related to hypoxia (29).

Further, after integrating the *Rh*- and AZ-regulated targets, the HIF-1α signaling pathway became more enriched. The false discovery rate dropped from $1.28\times E^{-20}$ in the AZ-enriched pathways and $1.37\times E^{-17}$ in the *Rh*-enriched pathways to $1.45\times E^{-23}$. In total, 39 *Rh*-related targets and 16 AZ-related targets were mapped to this pathway. However, after combining all the targets of *Rh* and AZ, the observed genes in this pathway increased to 48. This means that *Rh* and AZ not only share targets in this pathway but also have different targets. This further shows that they can regulate this pathway together. In *Figure 1*, the genes marked by a purple box are regulated by *Rh*, the genes marked by a black box are regulated by AZ, and the genes marked by a red box are regulated by both *Rh* and AZ. After integration, the number of targets regulated by *Rh* and AZ in this pathway increased.

Additionally, after integrating the targets regulated by *Rh* and AZ, the enriched pathways underwent subtle changes. As *Figure 1* shows, after integration, in addition to the shared pathways, the following 5 new purple pathways were added: glycolysis/gluconeogenesis (has00010), oxytocin signaling pathway (has04921), gap junction (has04540), viral myocarditis (has05416), and gonadotropin-releasing hormone (GnRH) signaling pathway (has04912).

The AS network was constructed by searching the CTD using the following keywords: "Altitude Sickness", "Brain Edema", "Hypoxia, Brain", "Hypoxia", "Hypoxia-Ischemia, Brain", "Polycythemia", "Pulmonary Arterial Hypertension", and "Pulmonary edema of mountaineers". The top 50 genes were found to be related to AS (see Table S3). Ultimately, 235 genes were selected to construct the AS network after removing the redundant data (see *Figure 2A*).

After mapping the *Rh*- and AZ-targeted proteins/genes into the AS network, we found that *Rh* modulated 86 proteins of AS (see *Figure 2B*), AZ modulated 16 proteins of AS (see *Figure 2C*), and together, *Rh* and AZ modulated 89 proteins of AS (see *Figure 2D*). Thus, *Rh* and AZ regulated most targets in the AS network. Further, excluding 3 different targets, *Rh* and AZ shared most of the targets. This evidence shows that when used in combination, *Rh* and AZ complement or enhance the regulation of high-altitude disease networks.

Rh and AZ reduced the expression of HIF-1α

The network pharmacology results showed that the HIF-1α signaling pathway was enriched by *Rh* and AZ. Additionally, the HIF-1α signaling pathway became more enriched after integration. We checked these results using RT-PCR. As *Figure 3* shows, the expression of HIF-1α significantly increased under hypoxia ($P<0.05$). However, the use of *Rh* and AZ reversed this increase, and they were more effective when used in combination than when used separately.

Rh and AZ improved the hemodynamics of rats under hypoxic conditions

In addition to the HIF-1α signaling pathway, 5 new pathways were found to be enriched after integrating the *Rh*- and AZ-related networks. Among them, oxytocin and GnRH signaling pathways are related to blood pressure. These hypotheses were confirmed by monitoring the hemodynamics in rats. We monitored 7 indices, including CVP, MAP, PAP, LAP, ABF, heart rate (HR), and Paw, under normoxia or hypoxia after treatment with *Rh* and AZ. As

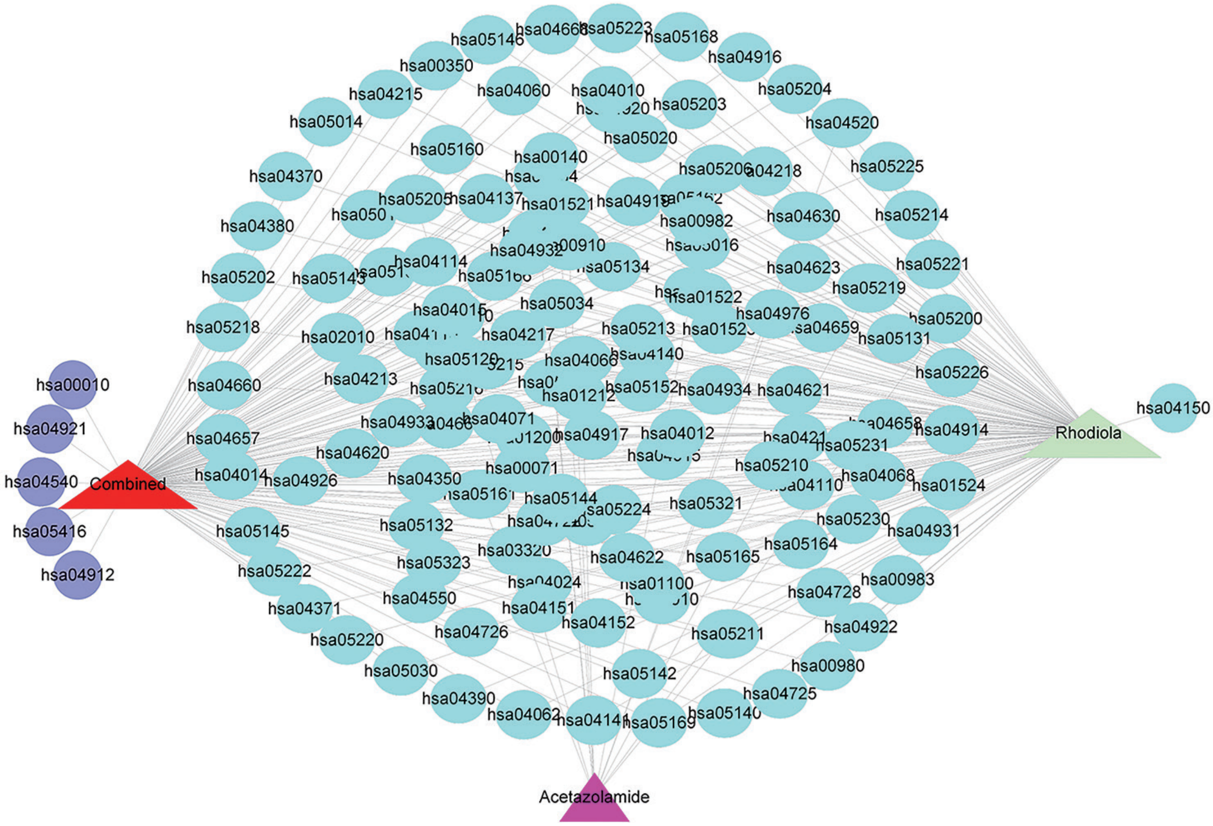

Figure 1 Drug-KEGG pathway interaction (the triangles represent drugs; the circles represent pathways; light blue indicates the co-regulated pathways; purple indicates the newly added pathways). KEGG, Kyoto Encyclopedia of Genes and Genomes.

Figure 4 and *Table 2* shown, a hypoxic environment led to an increase in PAP (37.2±2.0 to 39.9±2.5 mmHg) and LAP (2.5±0.2 to 2.7±0.1 mmHg), and a decrease in MAP (97.8±4.1 to 92.3±3.9 mmHg) and ABF (32.1±1.3 to 27.7±1.2 mmHg) in rats. However, *Rh* and AZ suppressed this change. The inhibitory effect was more obvious after their combined use, especially in relation to PAP, LAP, and ABF.

Conclusions

Rh and AZ are the two main drugs used to prevent and treat AS. In clinical practice, *Rh* is more commonly used to prevent AS, while AZ is more commonly used to treat AS. However, there are only a few clinical reports on their combined use. The mechanisms of the treatment and prevention of AS are not clear. In this study, we analyzed the mechanisms involved in the treatment and prevention of AS using the network pharmacology method. We verified the results of the experiments and found that *Rh* and AZ can alleviate the symptoms of AS by regulating HIF-1α and hemodynamics. Further, these drugs are more effective when they are used in combination than when they are used separately.

HIF-1α, a subunit of HIF-1, is expressed inducible according to the oxygen content (30). It undergoes degradation through hydroxylation at specific prolyl residues and subsequent ubiquitination under normoxia (31). Conversely, under hypoxia, HIF-1α becomes stable after interacting with its coactivators, such as p300/CBP (32-34). Eventually, HIF-1α encodes proteins that increase O_2 delivery and mediate adaptive responses to O_2 deprivation (35). In the present study, we found that *Rh* and AZ not only enriched the HIF-1 signaling pathway, but also suppressed HIF-1α gene expression. These effects became more pronounced when *Rh* and AZ were used in combination. Thus, reducing the expression of HIF-1α reduced the sensitivity of rat lung tissue to a hypoxic environment.

Collectively, *Rh* and AZ enriched 5 new pathways after their combined use. Among them, the oxytocin signaling pathway is related to the cardiovascular system

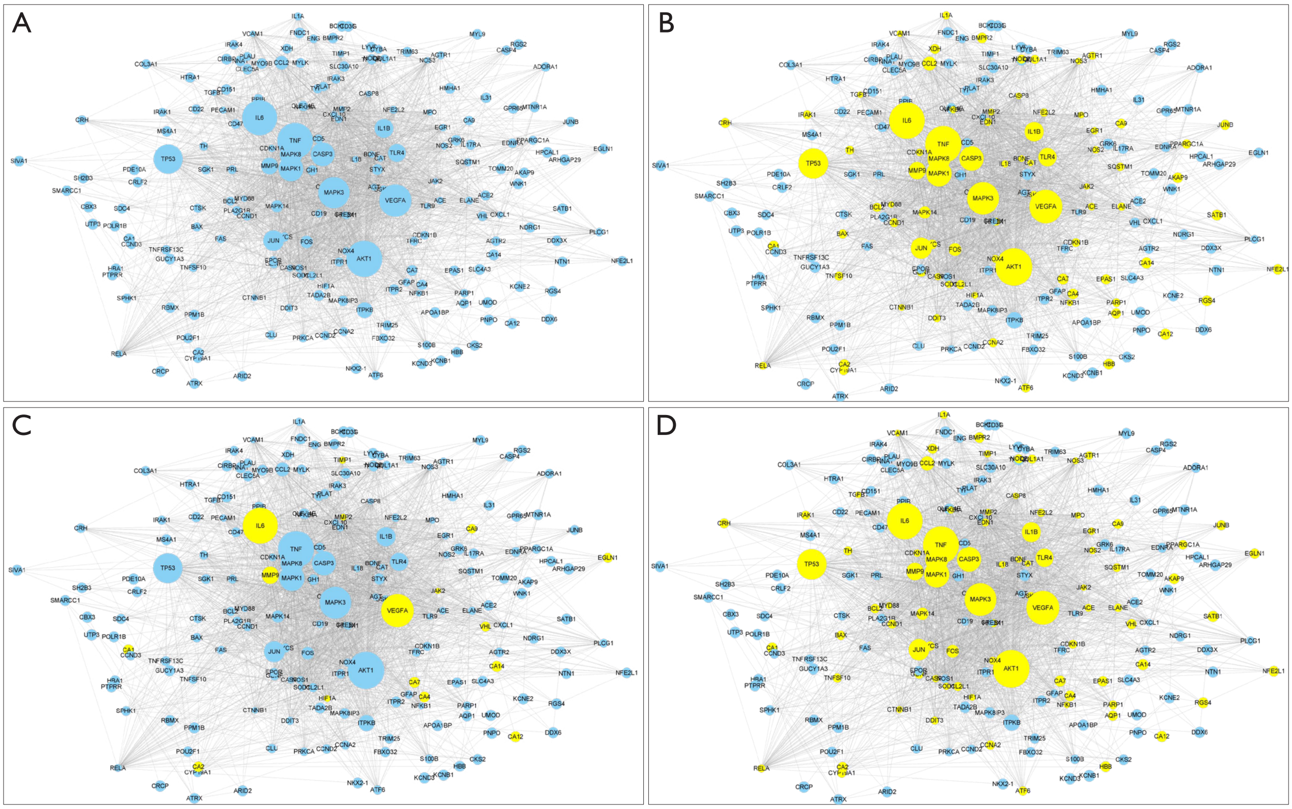

Figure 2 *Rh* and AZ regulate AS networks. (A) AS network. (B) The *Rh*-related protein targets presented in the AS network. (C) The AZ-related protein targets presented in the AS network. (D) The *Rh*- and AZ-related protein targets presented in the AS network. *Rh*, *Rhodiola*; AZ, acetazolamide; AS, altitude sickness.

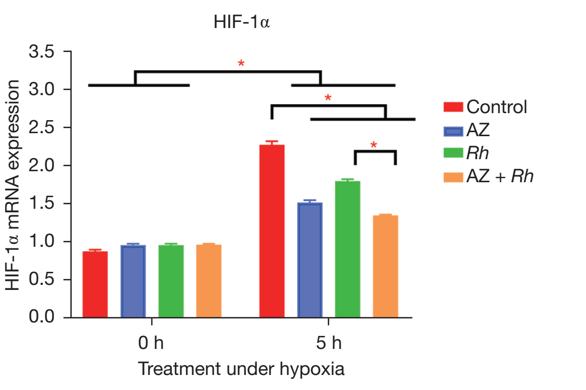

Figure 3 The expression of HIF-1α after treatment with *Rh* and AZ at normoxia and hypoxia. 0 h means the Rats were treated with normoxia and 5 h means the Rats were treated with hypoxia for 5 hours. The expression of HIF-1α was significantly increased under hypoxia. *Rh* and AZ inhibited this increase, and their combined use inhibited this increase more significant than alone use. *, P≤0.05. All data is presented mean ± SD. HIF, hypoxia-inducible factor; *Rh*, *Rhodiola*; AZ, acetazolamide.

(36,37). Oxytocin could reduce the force and rate of heart contraction and increase vasodilatation by mediating the atrial natriuretic peptide-Cyclic GMP (ANP-cGMP), and Nitric oxide-Cyclic GMP (NO-cGMP) pathways (38-40), which may reduce symptoms such as pulmonary hypertension or hypertension caused by AS (41). Additionally, in the GnRH signaling pathway, GnRH activates its receptor (GnRHR) in the anterior pituitary and subsequently activate phospholipase C by coupling with Gq/11 proteins (42). Activated phospholipase C further activates the intracellular protein kinase C (PKC) pathway, which in turn leads to the efflux of intracellular calcium (43). Eventually, such changes induce the dilation of epithelial cells, resulting in vasodilation (44,45). Based on these observations, we deduced that the pathways regulated by *Rh* and AZ were related to cardiovascular disease. These results were supported by our hemodynamic tests of rats. Specifically, we found that *Rh* and AZ suppressed changes in PAP, LAP, MAP, and ABF under hypoxia.

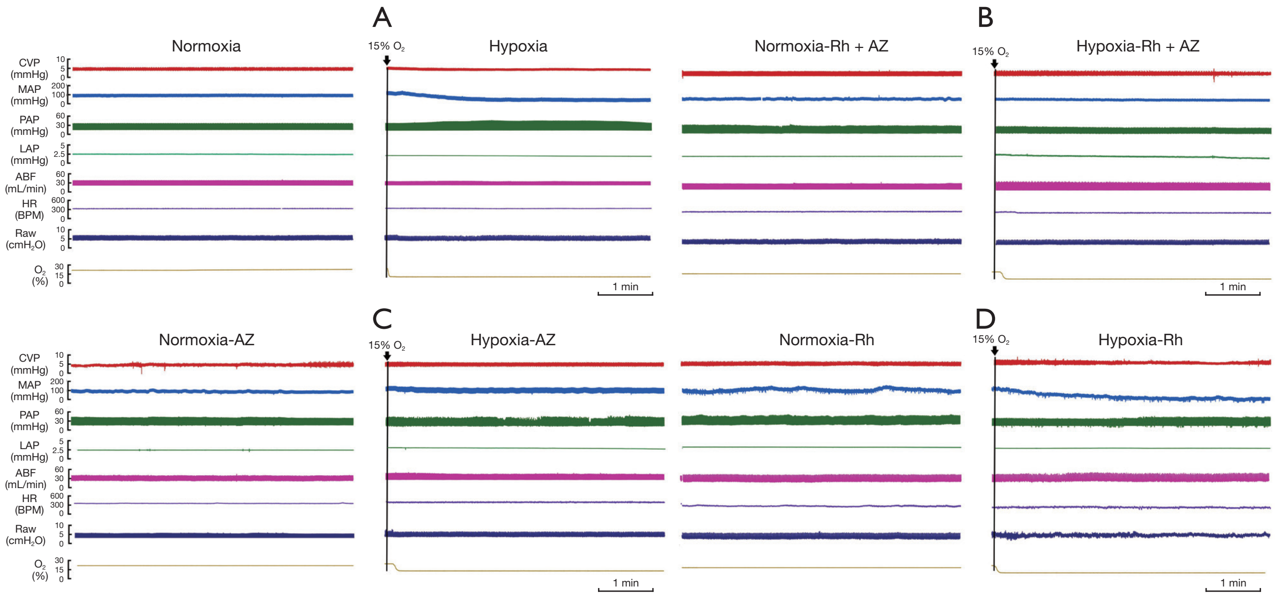

Figure 4 Hemodynamics of rats after treatment with *Rh* and AZ at normoxia and hypoxia. (A) Hemodynamic changes after normoxia and hypoxia treatment. (B) Hemodynamic changes after the combined treatment of *Rh* and AZ under the normoxia and hypoxia conditions. (C) Hemodynamic changes after treatment with AZ under the normoxia and hypoxia conditions. (D) Hemodynamic changes after treatment with *Rh* under the normoxia and hypoxia conditions. *Rh*, *Rhodiola;* AZ, acetazolamide.

Table 2 Results of the hemodynamic changes analysis in different groups of rats (n=6, mean ± SD)

Indexes	O_2	Control	AZ	*Rh*	AZ + *Rh*	F	P
CVP (mmHg)	20% O_2	4.3±0.2	4.3±0.3	4.1±0.3	4.0±0.4	1.23	0.32
	15% O_2	4.4±0.2	4.2±0.4	4.2±0.2	3.9±0.2*	4.25	0.02
MAP (mmHg)	20% O_2	97.8±4.1	96.1±3.2	96.7±3.4	96.4±3.6	0.30	0.82
	15% O_2	92.3±3.9#	94.6±3.5	95.1±4.1	96.1±3.3	1.31	0.29
PAP (mmHg)	20% O_2	37.2±2.0	36.9±2.0	37.3±2.4	37.1±2.5	0.04	0.98
	15% O_2	39.9±2.5#	37.8±2.5	37.9±0.35	37.3±0.03*	2.91	0.05
LAP (mmHg)	20% O_2	2.5±0.2	2.4±0.1	2.5±0.3	2.3±0.2	1.43	0.26
	15% O_2	2.7±0.1#	2.5±0.1*	2.6±0.3	2.4±0.1*	3.89	0.02
ABF ($mL{\cdot}min^{-1}$)	20% O_2	32.1±1.3	31.2±1.1	31.4±1.4	31.6±1.5	0.58	0.62
	15% O_2	27.7±1.2#	30.1±1.2*	29.8±1.2	30.7±1.3*	6.72	<0.01
Paw (cmH_2O)	20% O_2	10.7±0.6	10.2±0.4	10.6±0.3	10.4±0.5	1.60	0.21
	15% O_2	11.0±0.5	10.6±0.3	11.2±0.5	10.9±0.6	1.19	0.33
HR (bpm)	20% O_2	331±20.8	312±18.6	325±20.5	309±19.8	1.93	0.15
	15% O_2	334±19.3	323±17.4	330±18.1	316±19.2	1.28	0.3

*, *vs.* Control, P≤0.05; #, *vs.* Control 20% O_2, P<0.05. AZ, acetazolamide; *Rh*, *Rhodiola*; CVP, central venous pressure; MAP, mean arterial pressure; PAP, pulmonary artery pressure; LAP, left atrial pressure; ABF, ascending aortic blood flow; Paw, airway pressure; HR, heart rate.

Pulmonary hypertension caused by hypoxia is the most common cause of AS. Whether used alone or in combination, *Rh* and AZ can alleviate this symptom, and their combined effects are more pronounced than they are alone.

Based on the results of our research, the combined use of *Rh* and AZ helped to prevent and treat AS. However, while our results provide preliminary evidence of the potential clinical applicability of *Rh* and AZ in the treatment of AS, further clinical trials need to be conducted.

Acknowledgments

Funding: This study was supported by the National Natural Science Foundation of China (No. 81560301), the Natural Science Foundation of Qinghai (grant No. 2022-ZJ-905), and Qinghai Province "High-End Innovative Talents and Thousand Talents Program" Leading Talent Project. The High-Altitude Medicine Research Center of Qinghai University provided the experimental platform.

Footnote

Reporting Checklist: The authors have completed the ARRIVE reporting checklist. Available at https://atm.amegroups.com/article/view/10.21037/atm-22-2111/rc

Data Sharing Statement: Available at https://atm.amegroups.com/article/view/10.21037/atm-22-2111/dss

Conflicts of Interest: All authors have completed the ICMJE uniform disclosure form (available at https://atm.amegroups.com/article/view/10.21037/atm-22-2111/coif). The authors have no conflicts of interest to declare.

Ethical Statement: The authors are accountable for all aspects of the work in ensuring that questions related to the accuracy or integrity of any part of the work are appropriately investigated and resolved. The study was approved by the Medical Science Research Ethics Committee of Qinghai University School of Medicine (No. 2021-40), and animal handling and care procedures were conducted in accordance with institutional guidelines for the care and use of animals. All efforts were made to minimize pain and suffering to the animals and to minimize the number of animals used.

References

1. Luks AM, Swenson ER, Bärtsch P. Acute high-altitude sickness. Eur Respir Rev 2017;26:160096.
2. Jiang Y, Costello JT, Williams TB, et al. A network physiology approach to oxygen saturation variability during normobaric hypoxia. Exp Physiol 2021;106:151-9.
3. Carod-Artal FJ. High-altitude headache and acute mountain sickness. Neurologia 2014;29:533-40.
4. Marmura MJ, Hernandez PB. High-altitude headache. Curr Pain Headache Rep 2015;19:483.
5. Bärtsch P, Swenson ER, Paul A, et al. Hypoxic ventilatory response, ventilation, gas exchange, and fluid balance in acute mountain sickness. High Alt Med Biol 2002;3:361-76.
6. Jafarian S, Gorouhi F, Salimi S, et al. Sumatriptan for prevention of acute mountain sickness: randomized clinical trial. Ann Neurol 2007;62:273-7.
7. Semenza GL. Hypoxia and human disease-and the Journal of Molecular Medicine. J Mol Med (Berl) 2007;85:1293-4.
8. Chao J, Viets Z, Donham P, et al. Dexamethasone blocks the systemic inflammation of alveolar hypoxia at several sites in the inflammatory cascade. Am J Physiol Heart Circ Physiol 2012;303:H168-H177.
9. Tapia L, Irarrázaval S. Acetazolamide for the treatment of acute mountain sickness. Medwave 2019;19:e7737.
10. Toussaint CM, Kenefick RW, Petrassi FA, et al. Altitude, Acute Mountain Sickness, and Acetazolamide: Recommendations for Rapid Ascent. High Alt Med Biol 2021;22:5-13.
11. Shimoda LA, Suresh K, Undem C, et al. Acetazolamide prevents hypoxia-induced reactive oxygen species generation and calcium release in pulmonary arterial smooth muscle. Pulm Circ 2021;11:20458940211049948.
12. Gao D, Wang Y, Zhang R, et al. Efficacy of acetazolamide for the prophylaxis of acute mountain sickness: A systematic review, meta-analysis, and trial sequential analysis of randomized clinical trials. Ann Thorac Med

2021;16:337-46.
13. Abdeen A, Sonoda H, Oshikawa S, et al. Acetazolamide enhances the release of urinary exosomal aquaporin-1. Nephrol Dial Transplant 2016;31:1623-32.
14. Leaf DE, Goldfarb DS. Mechanisms of action of acetazolamide in the prophylaxis and treatment of acute mountain sickness. J Appl Physiol (1985) 2007;102:1313-22.
15. Swenson ER. Carbonic anhydrase inhibitors and high altitude illnesses. Subcell Biochem 2014;75:361-86.
16. Höhne C, Pickerodt PA, Francis RC, et al. Pulmonary vasodilation by acetazolamide during hypoxia is unrelated to carbonic anhydrase inhibition. Am J Physiol Lung Cell Mol Physiol 2007;292:L178-84.
17. Chiang HM, Chen HC, Wu CS, et al. Rhodiola plants: Chemistry and biological activity. J Food Drug Anal 2015;23:359-69.
18. Lee SY, Li MH, Shi LS, et al. Rhodiola crenulata Extract Alleviates Hypoxic Pulmonary Edema in Rats. Evid Based Complement Alternat Med 2013;2013:718739.
19. Jiang S, Deng N, Zheng B, et al. Rhodiola extract promotes longevity and stress resistance of Caenorhabditis elegans via DAF-16 and SKN-1. Food Funct 2021;12:4471-83.
20. Liu X, Ouyang S, Yu B, et al. PharmMapper server: a web server for potential drug target identification using pharmacophore mapping approach. Nucleic Acids Res 2010;38:W609-14.
21. Wang X, Shen Y, Wang S, et al. PharmMapper 2017 update: a web server for potential drug target identification with a comprehensive target pharmacophore database. Nucleic Acids Res 2017;45:W356-60.
22. Szklarczyk D, Gable AL, Lyon D, et al. STRING v11: protein-protein association networks with increased coverage, supporting functional discovery in genome-wide experimental datasets. Nucleic Acids Res 2019;47:D607-13.
23. Shannon P, Markiel A, Ozier O, et al. Cytoscape: a software environment for integrated models of biomolecular interaction networks. Genome Res 2003;13:2498-504.
24. Christou H, Michael Z, Spyropoulos F, et al. Carbonic anhydrase inhibition improves pulmonary artery reactivity and nitric oxide-mediated relaxation in sugen-hypoxia model of pulmonary hypertension. Am J Physiol Regul Integr Comp Physiol 2021;320:R835-R850.
25. Deng G, Jia S, Li J, et al. Experimental Study of Preventive Effect of Salidroside on Mice with High Altitude Polycythemia. Journal of New Chinese Medicine 2016;48:304-6.
26. Wang Q, Wang L, Wang P, et al. Protective effect of rhodiogenin on myocardium in rats with myocardia ischemia-reperfusion injury. Chinese Traditional Patent Medicine 2021;43:3147-51.
27. Ji Q, Zhang Y, Zhang H, et al. Effects of β-adrenoceptor activation on haemodynamics during hypoxic stress in rats. Exp Physiol 2020;105:1660-8.
28. Panossian A, Wikman G, Sarris J. Rosenroot (Rhodiola rosea): traditional use, chemical composition, pharmacology and clinical efficacy. Phytomedicine 2010;17:481-93.
29. Fu X, Zhang F. Role of the HIF-1 signaling pathway in chronic obstructive pulmonary disease. Exp Ther Med 2018;16:4553-61.
30. Yang C, Zhong ZF, Wang SP, et al. HIF-1: structure, biology and natural modulators. Chin J Nat Med 2021;19:521-7.
31. Kobayashi Y, Oguro A, Imaoka S. Feedback of hypoxia-inducible factor-1alpha (HIF-1alpha) transcriptional activity via redox factor-1 (Ref-1) induction by reactive oxygen species (ROS). Free Radic Res 2021;55:154-64.
32. Lee JW, Bae SH, Jeong JW, et al. Hypoxia-inducible factor (HIF-1)alpha: its protein stability and biological functions. Exp Mol Med 2004;36:1-12.
33. Qin X, Chen H, Tu L, et al. Potent Inhibition of HIF1α and p300 Interaction by a Constrained Peptide Derived from CITED2. J Med Chem 2021;64:13693-703.
34. Lanfranchi B, Rubia RF, Gassmann M, et al. Transcriptional regulation of HIF1α-mediated STAR expression in murine KK1 granulosa cell line involves cJUN, CREB and CBP-dependent pathways. Gen Comp Endocrinol 2022;315:113923.
35. Semenza GL. Hydroxylation of HIF-1: oxygen sensing at the molecular level. Physiology (Bethesda) 2004;19:176-82.
36. Chatterjee O, Patil K, Sahu A, et al. An overview of the oxytocin-oxytocin receptor signaling network. J Cell Commun Signal 2016;10:355-60.
37. Iovino M, Messana T, Tortora A, et al. Oxytocin Signaling Pathway: From Cell Biology to Clinical Implications. Endocr Metab Immune Disord Drug Targets 2021;21:91-110.
38. Jankowski M, Broderick TL, Gutkowska J. The Role of Oxytocin in Cardiovascular Protection. Front Psychol 2020;11:2139.
39. Szczepanska-Sadowska E, Wsol A, Cudnoch-Jedrzejewska A, et al. Complementary Role of Oxytocin and Vasopressin in Cardiovascular Regulation. Int J Mol Sci 2021;22:11465.

40. McCook O, Denoix N, Radermacher P, et al. H2S and Oxytocin Systems in Early Life Stress and Cardiovascular Disease. J Clin Med 2021;10:3484.
41. Broderick TL, Wang Y, Gutkowska J, et al. Downregulation of oxytocin receptors in right ventricle of rats with monocrotaline-induced pulmonary hypertension. Acta Physiol (Oxf) 2010;200:147-58.
42. Stamatiades GA, Kaiser UB. Gonadotropin regulation by pulsatile GnRH: Signaling and gene expression. Mol Cell Endocrinol 2018;463:131-41.
43. Maltsev AV, Evdokimovskii EV, Kokoz YM. Protein kinase C-mediated calcium signaling as the basis for cardiomyocyte plasticity. Arch Biochem Biophys 2021;701:108817.
44. Desaulniers AT, Cederberg RA, Lents CA, et al. Expression and Role of Gonadotropin-Releasing Hormone 2 and Its Receptor in Mammals. Front Endocrinol (Lausanne) 2017;8:269.
45. Muzorewa TT, Buerk DG, Jaron D, et al. Coordinated regulation of endothelial calcium signaling and shear stress-induced nitric oxide production by PKCβ and PKCη. Cell Signal 2021;87:110125.

(English Language Editor: L. Huleatt)

Cite this article as: Cao C, Zhang H, Huang Y, Mao Y, Ma L, Zhang S, Zhang W. The combined use of acetazolamide and *Rhodiola* in the prevention and treatment of altitude sickness. Ann Transl Med 2022;10(10):541. doi: 10.21037/atm-22-2111

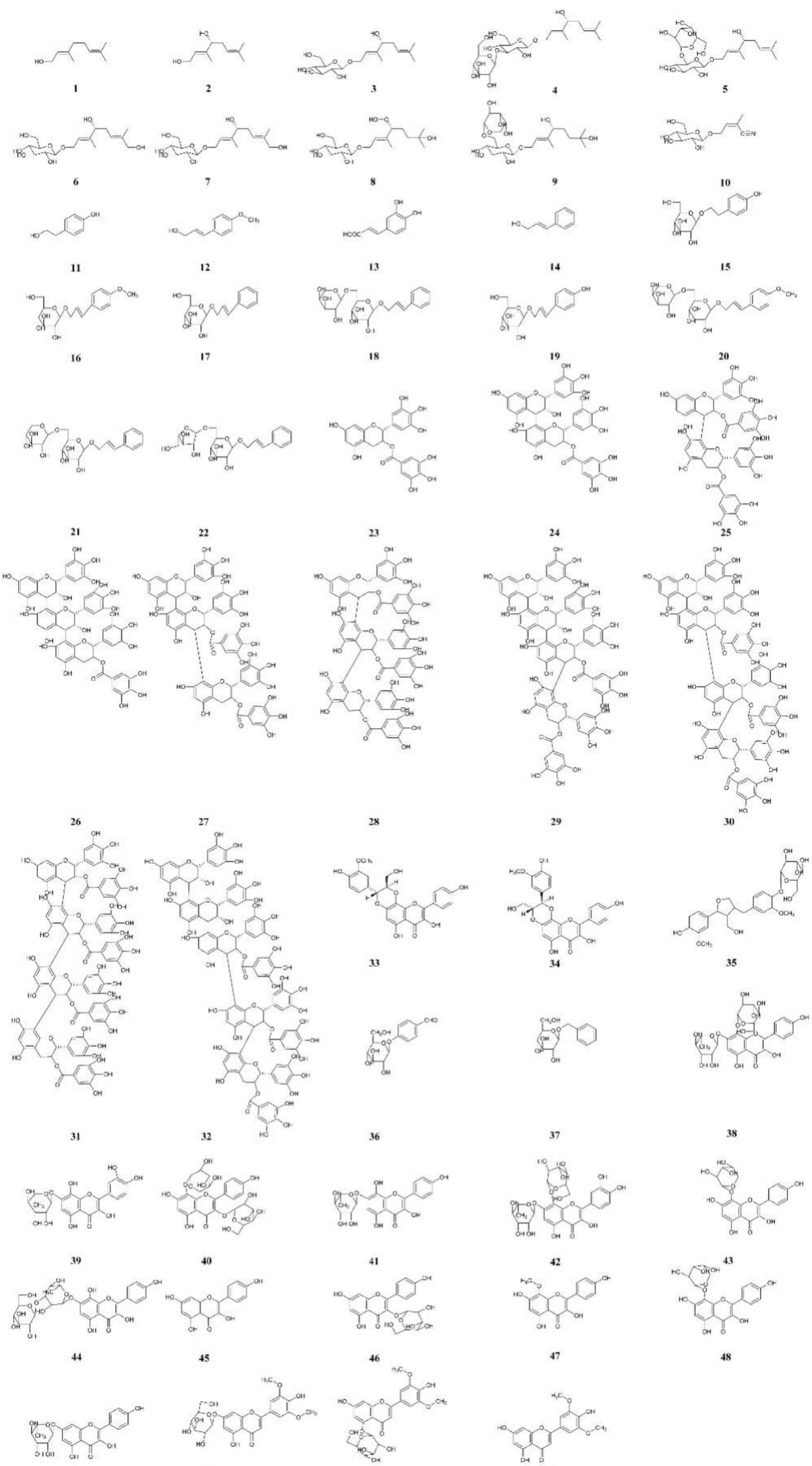

Figure S1 52 chemical components of *Rhodiola*.

https://dx.doi.org/10.21037/atm-22-2111

Table S1 The targets of the *Rhodiola*'s chemical constituents and acetazolamide

ID	Name	Targets
1	Geraniol	ESR1 ALOX15 ESR1 ABCC2 ACACA ACHE ACTA2 ACTL6A ACVR1 ADIPOQ AFF4 AGER AHCTF1 AKR1C1 AP5Z1 APBB2 APPL1 ARNTL ATF3 ATF4 ATF6 ATG12 ATG5 ATG7 BAK1 BAX BAZ1B BAZ2B BBX BCL11A BCL2 BCL2L1 BCL2L2 BCL6 BCLAF1 BDNF BIRC5 BMP6 BNIP3 BRCA1 BRCA2 BTF3 BUB1 BUB1B CASP3 CASP8 CASP9 CAT CBFA2T2 CBFB CCL4 CCNA2 CCNB1 CCND1 CD86 CDC20 CDC25A CDC25C CDC45 CDC7 CDH1 CDK1 CDK2 CDK4 CDKN1A CDKN1B CDKN2C CDKN3 CDT1 CEBPB CEBPG CENPE CENPF CHEK1 CIT CNBP CNGA2 COL1A1 COX7C CREB3 CREB3L2 CRP CTNNB1 CTSD CXCL8 CYB5A CYBB CYC1 CYP1A1 CYP1B1 CYP2B6 CYP2E1 CYP3A5 DBF4 DDIT3 DEK DMTF1 DNAJC1 DR1 DTYMK E2F1 E2F8 EHF EIF2AK3 EIF2S1 ELAVL2 ELF1 ELK4 ERC1 ERN1 ESPL1 ESR1 ESR2 ETS2 ETV1 EWSR1 EZH2 FABP4 FADS1 FANCG FASN FBXO5 FOS FOSL1 FOSL2 FOXA2 FOXJ3 FOXM1 FOXO4 FST FUBP1 G6PD GABRA1 GABRB1 GATAD1 GBX2 GCG GDNF GMNN GNA15 GNAL GOBP2 GPX1 GSK3B GSR GSTP1 GTF2B GTF2H1 GTF2IRD1 GTF3A GTF3C1 HAVCR1 HBB HBP1 HIVEP1 HLF HMBOX1 HMG20B HMGB2 HMGB3 HMGCR HMGXB3 HMGXB4 HMOX1 HNRNPAB HOXA5 HOXB13 HOXC6 HRAS HSPA2 HSTRPA HTR3A ICAM1 ID1 ID3 IFNG IL10 IL16 IL17A IL18 IL1A IL1B IL1R2 IL6 IL7R ILF2 INS1 IRF1 IRF6 IRF7 IRF9 JARID2 JMJD1C JUN JUNB JUND KDR KHDRBS1 KIF11 KIF15 KIF22 KIF23 KIF2C KLF11 KLF13 KLF3 KLF4 KLF5 KLF6 KLF7 KNTC1 KRAS KRBOX4 LCAT LDLR LIF LPL LZTFL1 LZTR1 MAD2L1 MAFF MAFG MAOA MAOB MAP2K1 MAPK1 MAPK3 MCM2 MEF2A MEN1 MKI67 MMP3 MNT MPO MTOR MVK MXD1 MXD4 MXI1 MYB MYBL1 MYBL2 MYO6 NASP NCAPH NCOR1 NDP NEK2 NFAT5 NFE2L1 NFE2L2 NFIL3 NFKB1 NFKBIA NFYB NOS2 NOX1 NPM1 NQO1 NR1D1 NR1D2 NR2F1 NR3C1 NR4A2 NSD2 NUSAP1 ODC1 OGG1 OLFR43 OR1A1 OR1G1 PA2G4 PBX1 PCNA PGR PHB PHF1 PHF21A PHTF1 PIK3R1 PKMYT1 PLAGL1 PLK1 POLA1 POLE POLR1G POR PPARA PPARG PRC1 PRDM4 PRDX3 PRKAA1 PTEN PTGS2 PTTG1 PWP1 RACGAP1 RAD51 RAD54B RAD54L RAF1 RCAN1 RCOR3 RELA RFX5 RNF19A RUVBL1 RUVBL2 SATB1 SERPINB3 SIM2 SIRT1 SKP2 SLC18A2 SLC2A4RG SLC6A3 SMAD3 SMAD6 SMAD7 SMARCA2 SMARCAL1 SMC4 SNCA SOD1 SOD2 SOX9 SP100 SP140L SQSTM1 SREBF1 SREBF2 STAT1 STAT2 STAT6 STMN1 SUB1 SUPT16H SUPT5H TARDBP TCEAL1 TCF12 TCF25 TCF4 TCF7L2 TERF1 TFAP2A TFCP2 TFDP1 TGFB1 TGIF1 TH TIMELESS TK1 TLE1 TLR4 TNF TP53 TPX2 TRAIP TRAK1 TRIM29 TRPS1 TRPV1 TSC22D3 TTK TULP3 TULP4 TYMS UBE2C UBE2N UBP1 UCP2 VCAM1 VEGFA VLDLR XBP1 ZBTB1 ZBTB10 ZBTB11 ZBTB20 ZHX2 ZMIZ1 ZMYM4 ZMYND11 ZNF134 ZNF165 ZNF189 ZNF195 ZNF207 ZNF211 ZNF224 ZNF23 ZNF248 ZNF263 ZNF264 ZNF274 ZNF281 ZNF304 ZNF329 ZNF331 ZNF334 ZNF354A ZNF394 ZNF410 ZNF44 ZNF467 ZNF468 ZNF557 ZNF571 ZNF589 ZNF606 ZNF611 ZNF75D ZNF768 ZNF84 ZSCAN16 ZSCAN18 ZSCAN31 ZSCAN5A ZZZ3 ABL2 AF1548 Acox1 Anxa5 DHRS1 EIF2B1 ERBB2 HB1 L2 MAGI2
2	Rosiridol	ABL2 ALOX12 Acox1 BRD7 DHRS1 ECH1 EIF2B1 ERBB2 Ets1 HB1
3	Rosiridin	ACR ALOX12 AVD CSDE1 CUL5 Cd3e DNMT1 EXOSC9 FES Flot2
4	Rhodiolosid B	ACR ALOX12 Anxa5 CELF4 CPSF3 CSDE1 DNMT1 EIF2S1 Flot2 Fnta
5	Rhodiolosid C	ACR ALOX12 Anxa5 CDC13 CELF4 CSDE1 ESA1 Fah Flot2 GBP1
6	Rhodiolosid A	ALOX12 Anxa5 CHI1 CSDE1 CUL5 DNMT1 EIL3 Flot2 Irf1 MT-CYB
7	Rhodiolosid D	CC0490 CPA4 CSDE1 ECE2 EEF1AKMT4 EEF1AKMT4-ECE2 Ets1 GOT2 NUCB1 PES1
8	Rhodiolosid El	ACS2 ALG13 Acox1 Anxa5 BCKDHA CSNK1G1 CTNNB1 DNMT1 GRK2 HHEX
9	Rhodiocyanoside A	ACAD8 ACO1 Anxa5 At1g07440 At1g07450 BMEI1586 CPSF3 ERBB2 FLNB HAO1
10	Lotaustralin	ACBD6 ACO1 ARO7 Anxa5 At1g07440 At1g07450 CPSF3 CUL5 KIFC3 Klk1b4
11	Tyrosol	CA5B hlyB CA5A CA2 ACS-2 AJM-1 AQP-2 B0024.4 B0228.6 BATH-10 C05B5.4 C06B8.7 C07D10.5 C08F1.10 C16H3.3 C17F4.7 C33D9.5 C33D9.6 C35E7.5 C39B5.2 C40A11.4 C49G7.12 CAV-1 CDC-14 CED-11 CEH-20 CEH-32 CEH-43 CEH-5 CES-2 CFZ-2 CHT-1 CKI-1 CLEC-196 CLEC-266 CLEC-60 CPG-20 CPG-24 CUTL-16 CUTL-20 CUTL-24 CUTL-29 CUTL-9 DLG-1 DPY-14 DSH-1 EEED8.15 EFL-3 EYA-1 F13E9.11 F20C5.6 F27C1.1 F35D2.3 F36H5.4 F36H5.8 F39E9.7 F40G9.5 F49E12.10 F53B3.5 F53C3.3 F55C9.3 F55C9.5 F57G12.1 F58A6.9 FBXB-101 FBXB-102 FBXB-66 FBXB-88 FBXC-40 FKH-8 FLP-15 FMI-1 G6PC1 G6PD GADR-3 GSP-3 HAM-1 HCH-1 HIL-7 HIS-24 HMG-6 IGCM-1 IGCM-3 IGCM-4 INS1 INS-2 IRG-2 K01A2.3 K05C4.9 K06A5.2 KLP-11 LAM-1 LAM-3 LPR-3 LTD-1 MLS-2 MLT-11 MNP-1 MPS-2 MSD-2 MSD-4 MSP-142 MSP-152 MSP-19 MSP-3 MSP-31 MSP-33 MSP-36 MSP-38 MSP-40 MSP-45 MSP-49 MSP-50 MSP-53 MSP-55 MSP-56 MSP-59 MSP-63 MSP-64 MSP-65 MSP-74 MSP-76 MSP-77 MSP-78 MSP-81 NAC-2 NCAM-1 NCX-3 NHR-11 NOAH-1 NOAH-2 NSPD-2 NSPD-4 ODC-1 PTGS2 PTP-4 PTR-22 RIG-5 RSF-1 SKR-21 SOX-2 SPTF-1 SQST-1 SQT-3 SSP-16 SSQ-3 T02E9.5 T09B4.5 T14B4.19 T28B8.1 T28D6.3 TBB-4 TIR-1 TLN-1 UNC-129 UNC-39 UNC-44 W03G11.4 W04A8.4 W05H12.2 WDFY-3 WRT-10 Y106G6G.4 Y110A2AL.4 Y11D7A.3 Y41D4A.3 Y43F8B.2 Y58A7A.4 Y58A7A.5 Y59H11AM.1 Y82E9BR.17 ZIG-4 ZIP-8 ZK512.1 Cgl3 ETR1 Ech1 GOT2 MAP2K2 MT-CYB NCBP1 SEC13 SENP7 SPEN
12	3-(4-Methoxyphenyl)-2-propen-1-ol	ACR AOC3 CDH-1 CDH-2 DDX50 EPN1 ERBB2 FBP1 GLR1 HDAC6
13	Caffeic acid	MMP9 MMP2 MMP1 CA2 GLS CA1 PTPN1 DPP4 CA7 CA5A CA6 CA9 GAA ALOX5 CA14 CA12 CA5B CA3 CA4 HDAC1 HDAC3 HDAC9 HDAC11 HDAC10 HDAC8 HDAC7 HDAC2 HDAC6 HDAC4 HDAC5 APP AKR1B1 ESR2 HSP90AB1 HSP90AA1 MCL1 GAPDH ALPL MPI GFER AKR1B10 NTMT1 ACACA ACHE ACLY ALOX15 ALOX5 ALPI ALT APP ARG1 ATP6V0D2 CASP3 CAT CCL2 CCL3 CCL4 CCR1 CCR2 CCR4 CD4 CD68 CDC20 CDK2 CHAT COMT COX2 CRH CTF1 CTSB CTSD CXCL2 CXCL8 CYP2E1 DAP DNAJB11 DPYSL4 EDN1 EGR1 ELMO2 ERF F3 FASN FLRT2 FLT4 G6PD GADD45A GLB1 GLS GOT1 GPT GSR GSTM1 GSTM2 GSTP1 GUSB H6PD HAVCR2 HES1 HLCS HMGCR HSP90B1 HSPE1 IFNG IL10 IL1B IL2 IL21R IL4 IL6 KCNN4 KIF15 KIF20B KIF2C LDHA LDHB MAOA MAOB MAP2K5 MAPK1 MAPK3 MFN1 MGST1 MPO MRPL45 MRRF NDP NOS2 NOS3 NOTCH1 NT5E PDCD10 PGD PIK3R1 PLK1 PLK4 PPARG PRDX5 PTGS2 PTX3 RAF1 RELA SCD1 SERPINE1 SFXN4 SLC2A4 SNCA SREBF1 STK32A SULT1A1 SULT1A2 SULT1A3 SULT1C2 TNF TP53 TYR UBE2C UGT1A10 UGT1A3 UGT1A7 UGT1A8 VEGFA XDH ACX1 ATIC DHRS4 GAS2 GTF2I LDHB PH1897 RUVBL1 Rab22a SEC13
14	Cinnamic alcohol	ABCB1 ABCB11 AKT1 ALPL BAX BCL2 BMP2 BMP6 BMP7 CASP1 CASP3 CAT CDH2 CERT1 CLDN11 CYP7A1 DDIT4 ENO2 FGF15 FN1 HES1 HIF1A MAP2 MTOR NGF NLRP3 NOG NOTCH1 NOX1 NOX2 NR0B2 NR1H4 OCLN PRKAR2B PYCARD RELA RPS6KB1 RUNX2 SIRT1 SMAD1 SMAD5 SMAD9 SOD2 SP7 SPP1 TGFB1 TJP1 TUBB3 TXNIP ACR AOC3 CDH-1 CDH-2 DDX50 Ddes2150 ERBB2 FBP1 GLR1 HDAC6 xynB xynD
15	Salidroside	ABCB1 ABCB11 AKT1 ALPL BAX BCL2 BMP2 BMP6 BMP7 CASP1 CASP3 CAT CDH2 CERT1 CLDN11 CYP7A1 DDIT4 ENO2 FGF15 FN1 HES1 HIF1A MAP2 MTOR NGF NLRP3 NOG NOTCH1 NOX1 NOX2 NR0B2 NR1H4 OCLN PRKAR2B PYCARD RELA RPS6KB1 RUNX2 SIRT1 SMAD1 SMAD5 SMAD9 SOD2 SP7 SPP1 TGFB1 TJP1 TUBB3 TXNIP Acox1 DDB1 DNMT1 Egr1 FGF1 HHEX KIFC3 Klk1b4 NUP214 PDE3B
16	Vimalin	ACAD8 ACBD6 ACS1 ALOX12 Ache BMEI1586 CNDP1 CPSF3 CSDE1 CTDSP2
17	Rosin	ACAD8 ACBD6 ACS1 AF1548 ALOX12 Ache BMEI1586 CHN2 CNDP1 CPSF3
18	Rosavin	EZH2 ACLY AQP1 AQP3 AR COX1 CYGB DSG3 EGF ESR2 FBN1 FBN2 FGF1 HAS1 HSPB1 IGF1 KL MC1R NOS2 NOS3 PGR PLOD3 POMC PPARG PTGER1 RAD23A RXRA SOD3 SRD5A2 TERT TPT1 TXN TYRP1 ACR AMA-1 Ache BT4395 CDH-1 CDH-2 CSDE1 DOCK9 FES GGH
19	Triandrin	ACAD8 ACBD6 Ache BMEI1586 CPSF3 CSDE1 CTDSP2 Chm DNMT1 FES
20	4-Methoxycinnamyl 6-O-alpha-L-arabinopyranosyl-b-D-glucopyranoside	ACAD8 ACR Ache Anxa5 BT4395 CCNE1 CSDE1 GGH MJ0882 NF2
21	Cinnamyl 6-O-beta-D-xylopyranosyl-beta-D-glucopyranoside	ACR Ache Acox1 Anxa5 BT4395 CCNE1 CDH-1 CDH-2 CSDE1 DPYS
22	Rosarin	ACR Ache Acox1 Anxa5 CCNE1 CDH-1 CDH-2 CSDE1 ESRRB FES
23	EGCG	ABCB1 BCL2 NFE2L2 DYRK1A TTR POLB PGAM1 DNMT1 APP STAT1 PGD BACE1 HIF1A DHFR DHFRP1 TERT MAPKAPK5 MAPT PTGES MAPK14 MET PKM GAA JUN MMP14 BAZ2B MMP2 GALK1 DPP4 NFKB1 ELANE MEN1 KMT2A ESR1 PIN1 GLI3 MMP7 TP53 NR1I3 TSHR AR THRB EP300 CNR1 PPARG ATF6 CREBBP FASN ESRRA KAT2B KAT5 HSP90AB1 ABCB11 BCL2L10 BCL2L1 BCL2L2 NCOA3 MCL1 NCOA1 BCL2A1 NCF1 PTGER2 GNAO1 RGS16 RGS8 RGS7 RGS19 RGS4 MAPK1 RAD51 SLC12A5 LMNA MAP3K3 MAP4K2 NPSR1 KLF5 NPBWR1 RGS12 GNAI1 GLA GBA BLM MBNL1 KCNH2 GAPDH GSK3B S1PR3 WEE1 NPY2R NPY1R HSP90AA1 RBBP9 VCP MCOLN3 S1PR4 EIF2AK3 JAK2 SLC6A3 ALPL X MPI DLD CACNA1B KCNQ1 CBFB RUNX1 NOD2 PTPN22 OPRK1 UBE2N NOD1 DUSP3 GPR55 CTNNB1 PHOSPHO1 PLEC TNFSF10 SENP6 EIF4H ALPI APLNR SENP8 UBE2I UBA2 SAE1 NLRP1 NLRP3 SENP7 GPR35 FKBP1A EIF4G1 CACNA1H RXFP1 PTGS2 PTGS1 EPAS1 USP2 RAB9A DRD2 NPC1 MDM4 MDM2 EYA2 ADRB2 APOBEC3A APOBEC3G TRHR KAT2A NTSR1 DRD1 APAF1 CCT2 TRPV1 NR3C1 VDR NR1H4 RXRA PPARD ALB AHR PPARA NR1I2 NRP2 ATAD5 CYP19A1 RARA vif HDAC9 MITF ESR2 KCNJ6 YAP1 AKR1B10 ERBB2 RPSA PGR SMAD3 SMAD2 CGAS CASP3 CASP7 HSF1 SLCO1B3 SLCO1B1 ACE ICAM1 AAMDC AAR2 AASDH ABCA1 ABCB1 ABCB10 ABCB11 ABCC1 ABCC10 ABCC2 ABCC4 ABCC5 ABCD3 ABCE1 ABCG1 ABCG2 ABHD6 ABL2 ABR ACACA ACADM ACADSB ACAP2 ACAT2 ACE ACLY ACOT13 ACSL1 ACSS2 ACTA2 ACTB ACTBL2 ACTR10 ADAM19 ADAM20 ADAMTS12 ADAMTS15 ADAMTS4 ADAMTS5 ADAMTSL4-AS1 ADARB1 ADAT1 ADGRE1 ADM ADRA1B ADRB2 ADSS ADSS2 AFF1 AFG1L AGAP1 AGER AGL AGPS AGTR1 AHCY AHR AIDA AIFM1 AIMP1 AJUBA AKAP13 AKAP9 AKIP1 AKIRIN2 AKR1C1 AKR1C2 AKR1C3 AKT1 AKT3 AKTIP ALDH3A2 ALDOA ALDOC ALG14 ALG6 ALG8 ALPK2 AMH AMMECR1 AMPD1 ANAPC10 ANAPC4 ANAPC7 ANKIB1 ANKMY2 ANKRD10 ANKRD26 ANKRD36 ANKRD44 ANO1 ANO4 ANO6 ANXA11 ANXA4 AOPEP AP1S3 AP2A2 AP5S1 APAF1 ACR ATIC Ache Alad CAPN9 CCNE1 CSDE1 CUL5 Flot2 HA
24	EGC-EGCG	ALOX12 AZGP1 Alad CSDE1 Cyb5a EIF4A1 F13A1 FUT8 Flot2 GAL10
25	2EGCG	ACBD7 ALOX12 Ache CITED2 Capn2 MKI67 NXT1 PAB1 PH0601 PRPS1
26	2EGC-EGCG	ACX1 ARHGAP11A ARHGEF12 CDC4 CITED2 CSDE1 CUL1 CYP2C5 Cnot4 F13A1
27	EGC-2EGCG	ACBD7 CPK1 CSDE1 CUL1 CUL5 EIF4A1 EP300 GAL10 GOT1 IL10RA
28	3EGCG	yhfA yxaF ARHGAP11A AZGP1 Alad CDC13 CKX7 CSDE1 Capn2 Dab1
29	2EGC-2EGCG	ACADVL ACX1 ARHGAP11A CSDE1 Grin3a HSD11B1 Ighg1 MMP2 RGS6 SERPING1
30	EGC-3EGCG	
31	4EGCG	
32	2EGC-3EGCG	ACR AR AZGP1 CBL4 CLPP CPK1 CSDE1 CUL1 GAL10 GOT1
33	Rhodiolin	CEP3 CLIC2 CPSF3 Cyb5b FKBP4 HB1 HD1794 L2 NUP214 PAL
34	(2R,3R)-6,8-dihydroxy-2-(4-hydroxy-3-methoxyphenyl)-3-(hydroxymethyl)-9-(4-hydroxyphenyl)-2,3-dihydro-7H-(1,4)dioxino(2,3-h)chromen-7-one	ACADVL CAM CEP3 CLCNKA CPSF3 DHRS1 Ets1 GCDH H2-Ea Musk
35	(2R,3S,4R,5R,6S)-2-(4-((5-(4-hydroxy-3-methoxyphenyl)-4-(hydroxymethyl)tetrahydrofuran-3-yl)methyl)-2-methoxyphenoxy)-6-(hydroxymethyl)tetrahydro-2H-pyran-3,4,5-triol	ACR ALOX12 BT4395 CDC19 CPB2 CSDE1 Dlg1 Gcm1 H2-K1 MID1
36	4-(((2S,3R,4S,5S,6R)-3,4,5-Trihydroxy-6-(hydroxymethyl)tetrahydro-2H-pyran-2-yl)oxy)benzaldehyde	ACO1 At1g07440 At1g07450 BMPR2 CKX7 CPSF3 CST7 DMD FN1 FOL1
37	Benzyl beta-d-glucopyranoside	ACBD6 ACO1 At1g07440 At1g07450 CPSF3 FGA HAO1 IGF1R KIFC3 Klk1b4
38	3,5-dihydroxy-2-(4-hydroxyphenyl)-8-(((2R,3R,4S,5S,6S)-3,4,5,6-tetrahydroxytetrahydro-2H-pyran-2-yl)oxy)-7-(((2S,3R,4R,5R,6S)-3,4,5-trihydroxy-6-methyltetrahydro-2H-pyran-2-yl)oxy)-4H-chromen-4-one	CSDE1 DPYS EPHB2 FAS2 GOT1 LYS3 MAGI1 MID1 Ngly1 PES1
39	Rhodiolgin	ACR AMA-1 COG2 CRS2 CSDE1 EXOSC9 F13A1 FAS2 GAN Nlgn1
40	5,7-dihydroxy-2-(4-hydroxyphenyl)-3-((3,4,5-trihydroxy-6-(hydroxymethyl)tetrahydro-2H-pyran-2-yl)oxy)-8-((3,4,5-trihydroxytetrahydro-2H-pyran-2-yl)oxy)-4H-chromen-4-one	Acox1 DNMT1 Fah GPD1L HAO1 HHEX MT-CYB PCNA PMP2 RAB31
41	Rhodionin	ACR Anxa5 CSDE1 Cyt-b5 DDX58 Fah GAN GOT1 HGD MYD88
42	2-(3,4-dihydroxyphenyl)-3,5-dihydroxy-8-((3,4,5-trihydroxy-6-(hydroxymethyl)tetrahydro-2H-pyran-2-yl)oxy)-7-(((2S,3R,4R,5R,6S)-3,4,5-trihydroxy-6-methyltetrahydro-2H-pyran-2-yl)oxy)-4H-chromen-4-one	EPHB2 Echs1 HBP1 MAP2K6 PES1 RUVBL1 SLC30A9 VC1409 VTC2 Vcp
43	3,5,7-trihydroxy-2-(4-hydroxyphenyl)-8-((3,4,5-trihydroxytetrahydro-2H-pyran-2-yl)oxy)-4H-chromen-4-one	ACADS ASS1 Acox1 CC0490 CPSF3 Cyb5r3 DNAJC30 Egr1 FGA HB1
44	7-((3,5-dihydroxy-6-methyl-4-(((2S,3R,4S,5S,6R)-3,4,5-trihydroxy-6-(hydroxymethyl)tetrahydro-2H-pyran-2-yl)oxy)tetrahydro-2H-pyran-2-yl)oxy)-3,5,8-trihydroxy-2-(4-hydroxyphenyl)-4H-chromen-4-one	ARSA COMTD1 DBT DSP FAS2 GAS2 GPH1 MAGI1 MID1 PES1
45	Kaempferol	CA7 AHR CYP1B1 CISD1 CA12 HSD17B2 DPP4 CYP1A1 CYP1A2 CSNK2B CSNK2A1 CSNK2A2 TYR HSD17B1 XDH NOX4 Dyrk1a Akr1b1 HIF1A ALOX15 MPO FLT3 ABCC1 ALOX5 GSK3B GSK3A SLC2A1 ABCG2 PGR CYP2C9 Abcb1a ABCB1 ESR1 Sialidase CA2 ESRRA ESR2 AR CTDSP1 CYP2D6 DAPK1 MAPT HDAC9 BACE1 CYP3A4 RARA Enoyl GLO1 GLI3 NFE2L2 CDK6 POLH HPGD LOC116160065 NR1I3 CCNB3 CDK1 CCNB2 CCNB1 NR1I2 Neuraminidase BCHE RACGAP1 POLI PIM2 CLK1 STK16 Syk Plcg2 Plcg1 PAFAH1B3 CHRM1 Prkaa2 Pparg RdRp PIP4K2A daf ADAM10 ADAM17 SIAE NR3C1 CYP19A1 PNLIP SMAD3 SMAD2 APP NFKB1 RELA NFKB2 ABCB1 ABCC1 ACHE ACTA2 AFP AHR AIP AKT1 ALOX12 ALOX5 APOE APP AR ARNT ATM B3GALT5 BAX BBC3 BCL2 BCL2A1 BCL2L1 BMP2 BMP4 CALCR CASP1 CASP3 CASP9 CAT CCKAR CCL2 CCL5 CCN5 CCNB1 CCND1 CD14 CD44 CDK1 CDKN1A CDKN2C CFTR CHEK1 CHEK2 CHUK COL10A1 COL2A1 CPT1A CRP CS CSF2 CTNNB1 CXCL8 CYCB CYCS CYP1A1 CYP1A2 CYP1B1 CYP2C9 CYP2E1 CYP3A4 DHRS11 DHRS4 DIO2 DUOX1 EP300 ESR1 ESR2 FBP1 FN1 FOS GADD45B GCLC GPT GREB1 GSK3B GSTA1 GSTM2 GSTP1 H2AX HBB HCAR2 HGF HIF1A HMOX1 ICAM1 IFNG IL1B IL32 IL4 IL5 IL6 INS1 IRAK1 ITGAM JUN KMT2A LAMB2 MAP3K7 MAPK1 MAPK3 MAPK8 MAPK9 MET MMP2 MOD2 MT2A MUC5AC NANOG NCOA3 NFE2L2 NFKBIA NOS2 NOX4 NQO1 NR1I2 NR1I3 OCLN PARP1 PCNA PGR POU5F1 PPARG PPARGC1A PSCA PTGES PTGS2 PYCARD RELA RIPK1 RPA3 RUNX2 SELE SFN SLC16A1 SLC2A1 SLC2A4 SLC5A8 SLCO1B1 SLCO1B3 SLCO2B1 SOD1 SOD2 SOX9 SPP1 STAT1 STAT2 TFAM TFF1 TGFA TJP1 TK1 TNF TNFAIP3 TNFRSF11A TNFSF11 TP53 TP53I3 TP63 TP73 TRAF6 TSLP TUBB3 UCP1 UCP3 UGT1A1 UGT1A10 UGT1A3 UGT1A7 UGT1A8 UGT1A9 UTRN VCAM1 VDR VEGFA XDH ADAM17 BLVRA CPSF3 ERBB4 FLNB FUT8 Flot2 HSPA8 NUP214 PRO2
46	Kaempferol 3-O-beta-L-glucopyranoside	P4HB GSK3A GFER CRS2 ECI1 EXOSC9 GID1A IMPDH KAP95 NCF2 PAL PAP1 PRP24
47	Sexangularetin	ACADS ACX1 ADAM17 At1g07440 At1g07450 BLVRA CUEDC1 ECH1 ERBB4 FLNB
48	3,5,7-trihydroxy-2-(4-hydroxyphenyl)-8-((3,4,5-trihydroxytetrahydro-2H-pyran-2-yl)oxy)-4H-chromen-4-one	ADAM17 Acox1 CC0490 CPSF3 CTDSP2 CUL5 Cyb5r3 DNAJC30 DSL1 FGA
49	Kaempferol-7-rhamnoside	ALAD BLVRA Cyb5a Cyb5b Ets1 GOT1 HGD Ighg1 MYD88 NCALD
50	5-hydroxy-2-(4-hydroxy-3,5-dimethoxyphenyl)-7-((3,4,5-trihydroxy-6-(hydroxymethyl)tetrahydro-2H-pyran-2-yl)oxy)-4H-chromen-4-one	CHI1 DPEP DSP EPHB2 GALM HAO1 LDHB RAB31 RNF8 RORA
51	7-hydroxy-2-(4-hydroxy-3,5-dimethoxyphenyl)-5-((3,4,5-trihydroxy-6-(hydroxymethyl)tetrahydro-2H-pyran-2-yl)oxy)-4H-chromen-4-one	ACR Ache Acox1 CST7 DEK DSP FAS2 HAO1 HECTD1 Lhx3
52	Tricin	AKR1B1 PTGS1 PTGS2 Acox1 DRAP1 Ets1 FUT8 Flot2 GOT2 GRB14 HSPA8 MJ0158
	Acetazolamide	CA11 CA6 CA14 CA2 CA4 CA12 CA5B CA13 CA1 CA5A CA9 CA7 CA3 AQP4 MMP12 MMP2 ACAN ARNT COL18A1 CREBBP CTNND1 DCN EGFR EGLN1 EP300 FLT1 FYN HIF1A HIF1AN IL6 JAK1 JAK2 KDR MMP14 MMP9 NRP2 PXN SRC STAT3 TCEB1 TCEB2 TIMP1 TIMP2 TIMP3 VEGFA VHL SCN4A GH-LCR CACNA1A CA2 CACNA1S CA1 SLC2A1 KCNA2 CA14 DARS2 EA3 CACNB4 SCN2A SLC1A3 BPPV KCNA1 CA12 KCNJ2 PIGT CA5B PDHA1 GLUT1 DEE32 ASPRS. LBSL CACNL1A3 EJM6 SCN2A1 EAAT1 AEMK HYPP HHIRK1 CACNL1A4 NDAP PHE1A HTLVR CCHL1A3 EA5 BFIC3 EA6 EA1 NAC1A KIR2.1 SCA6 PNH2 PDHAD DYT18 TTPP1 EIG9 DEE11 HOKPP2 IRK1 DEE42 MCAHS3 PED HOKPP1 BFIS3 CMS16 LQT7 GLUT1DS MHS5 BFNIS SQT3 EIG12 EA9 ATFB9 DYT9 SDCHCN

 https://dx.doi.org/10.21037/atm-22-2111

Table S2 Enriched KEGG pathways (false discovery rate <E^{-05})

Rhodiola		Acetazolamide		Combined	
Term ID	Term description	#term ID	Term description	#term ID	Term description
hsa05200	Pathways in cancer	hsa00910	Nitrogen metabolism	hsa05200	Pathways in cancer
hsa05418	Fluid shear stress and atherosclerosis	hsa04066	HIF-1 signaling pathway	hsa05418	Fluid shear stress and atherosclerosis
hsa05161	Hepatitis B	hsa05211	Renal cell carcinoma	hsa05161	Hepatitis B
hsa04068	FoxO signaling pathway	hsa05200	Pathways in cancer	hsa04068	FoxO signaling pathway
hsa05215	Prostate cancer	hsa05205	Proteoglycans in cancer	hsa05215	Prostate cancer
hsa04933	Advanced glycation end products-receptor for advanced glycation end products (AGE-RAGE) signaling pathway in diabetic complications	hsa01521	EGFR tyrosine kinase inhibitor resistance	hsa04933	AGE-RAGE signaling pathway in diabetic complications
hsa04110	Cell cycle	hsa05167	Kaposi's sarcoma-associated herpesvirus infection	hsa04110	Cell cycle
hsa05206	MicroRNAs in cancer	hsa04520	Adherens junction	hsa05206	MicroRNAs in cancer
hsa04066	HIF-1 signaling pathway	hsa05219	Bladder cancer	hsa04066	HIF-1 signaling pathway
hsa05203	Viral carcinogenesis	hsa05161	Hepatitis B	hsa05203	Viral carcinogenesis
hsa05166	HTLV-I infection	hsa05206	MicroRNAs in cancer	hsa05166	HTLV-I infection
hsa05167	Kaposi's sarcoma-associated herpesvirus infection	hsa04630	Jak-STAT signaling pathway	hsa05167	Kaposi's sarcoma-associated herpesvirus infection
hsa04210	Apoptosis	hsa04510	Focal adhesion	hsa04210	Apoptosis
hsa05202	Transcriptional misregulation in cancer			hsa05202	Transcriptional misregulation in cancer
hsa05212	Pancreatic cancer			hsa05212	Pancreatic cancer
hsa04010	Mitogen-activated protein kinase (MAPK) signaling pathway			hsa04010	MAPK signaling pathway
hsa04668	Tumor necrosis factor (TNF) signaling pathway			hsa04668	TNF signaling pathway
hsa05162	Measles			hsa05162	Measles
hsa01522	Endocrine resistance			hsa01522	Endocrine resistance
hsa05165	Human papillomavirus infection			hsa05165	Human papillomavirus infection
hsa04380	Osteoclast differentiation			hsa04380	Osteoclast differentiation
hsa04151	Phosphatidylinositol 3' -kinase (PI3K-Akt) signaling pathway			hsa04151	PI3K-Akt signaling pathway
hsa05210	Colorectal cancer			hsa05210	Colorectal cancer
hsa04218	Cellular senescence			hsa04218	Cellular senescence
hsa04657	Interleukin 17 (IL-17) signaling pathway			hsa04657	IL-17 signaling pathway
hsa05225	Hepatocellular carcinoma			hsa05225	Hepatocellular carcinoma
hsa04064	Nuclear factor-kappa B (NF-kappa B) signaling pathway			hsa04064	NF-kappa B signaling pathway
hsa05169	Epstein-Barr virus infection			hsa05169	Epstein-Barr virus infection
hsa05142	Chagas disease (American trypanosomiasis)			hsa05142	Chagas disease (American trypanosomiasis)
hsa05164	Influenza A			hsa05164	Influenza A
hsa05224	Breast cancer			hsa05224	Breast cancer
hsa04659	Th17 cell differentiation			hsa04659	Th17 cell differentiation
hsa05145	Toxoplasmosis			hsa05145	Toxoplasmosis
hsa05152	Tuberculosis			hsa05152	Tuberculosis
hsa04621	Nucleotide-binding and oligomerization domain (NOD)-like receptor signaling pathway			hsa04621	NOD-like receptor signaling pathway
hsa01521	Epidermal growth factor receptor (EGFR) tyrosine kinase inhibitor resistance			hsa01521	EGFR tyrosine kinase inhibitor resistance
hsa04919	Thyroid hormone signaling pathway			hsa04919	Thyroid hormone signaling pathway
hsa05134	Legionellosis			hsa05134	Legionellosis
hsa05220	Chronic myeloid leukemia			hsa05220	Chronic myeloid leukemia
hsa05205	Proteoglycans in cancer			hsa05205	Proteoglycans in cancer
hsa04620	Toll-like receptor signaling pathway			hsa04620	Toll-like receptor signaling pathway
hsa05218	Melanoma			hsa05218	Melanoma
hsa04115	*p53* signaling pathway			hsa04115	p53 signaling pathway
hsa05214	Glioma			hsa05214	Glioma
hsa05133	Pertussis			hsa05133	Pertussis
hsa04914	Progesterone-mediated oocyte maturation			hsa04914	Progesterone-mediated oocyte maturation
hsa04926	Relaxin signaling pathway			hsa04926	Relaxin signaling pathway
hsa05223	Non-small cell lung cancer			hsa05223	Non-small cell lung cancer
hsa05160	Hepatitis C			hsa05160	Hepatitis C
hsa04915	Estrogen signaling pathway			hsa04915	Estrogen signaling pathway
hsa05219	Bladder cancer			hsa05219	Bladder cancer
hsa05222	Small cell lung cancer			hsa05222	Small cell lung cancer
hsa05140	Leishmaniasis			hsa05140	Leishmaniasis
hsa05221	Acute myeloid leukemia			hsa05221	Acute myeloid leukemia
hsa05226	Gastric cancer			hsa05226	Gastric cancer
hsa04660	T cell receptor signaling pathway			hsa04660	T cell receptor signaling pathway
hsa05211	Renal cell carcinoma			hsa05211	Renal cell carcinoma
hsa04917	Prolactin signaling pathway			hsa04917	Prolactin signaling pathway
hsa05213	Endometrial cancer			hsa05213	Endometrial cancer
hsa01524	Platinum drug resistance			hsa01524	Platinum drug resistance
hsa04350	transforming growth factor-beta (TGF-beta) signaling pathway			hsa04350	TGF-beta signaling pathway
hsa04932	Non-alcoholic fatty liver disease (NAFLD)			hsa04932	Non-alcoholic fatty liver disease (NAFLD)
hsa05168	Herpes simplex infection			hsa05168	Herpes simplex infection
hsa04722	Neurotrophin signaling pathway			hsa04722	Neurotrophin signaling pathway
hsa01100	Metabolic pathways			hsa01100	Metabolic pathways
hsa04140	Autophagy—animal			hsa04140	Autophagy—animal
hsa05132	Salmonella infection			hsa05132	Salmonella infection
hsa05230	Central carbon metabolism in cancer			hsa05230	Central carbon metabolism in cancer
hsa04550	Signaling pathways regulating pluripotency of stem cells			hsa04550	Signaling pathways regulating pluripotency of stem cells
hsa05321	Inflammatory bowel disease (IBD)			hsa05321	Inflammatory bowel disease (IBD)
hsa04920	Adipocytokine signaling pathway			hsa04920	Adipocytokine signaling pathway
hsa04012	Receptor tyrosine-protein kinase erbB (ErbB) signaling pathway			hsa04012	ErbB signaling pathway
hsa04211	Longevity regulating pathway			hsa04211	Longevity regulating pathway
hsa04371	Apelin signaling pathway			hsa04371	Apelin signaling pathway
hsa04024	Cyclic adenosine 3', 5'-monophosphate (cAMP) signaling pathway			hsa04024	cAMP signaling pathway
hsa00140	Steroid hormone biosynthesis			hsa00140	Steroid hormone biosynthesis
hsa04060	Cytokine-cytokine receptor interaction			hsa04060	Cytokine-cytokine receptor interaction
hsa04664	Receptor for the Fc region of IgE(Fc epsilon RI) signaling pathway			hsa04664	Fc epsilon RI signaling pathway
hsa05034	Alcoholism			hsa05034	Alcoholism
hsa05216	Thyroid cancer			hsa05216	Thyroid cancer
hsa04630	Janus kinase/signal transducers and activators of transcription (Jak-STAT) signaling pathway			hsa04630	Jak-STAT signaling pathway
hsa05204	Chemical carcinogenesis			hsa05204	Chemical carcinogenesis
hsa04137	Mitophagy—animal			hsa04137	Mitophagy—animal
hsa05323	Rheumatoid arthritis			hsa05323	Rheumatoid arthritis
hsa04931	Insulin resistance			hsa04931	Insulin resistance
hsa04520	Adherens junction			hsa04520	Adherens junction
hsa04370	Vascular endothelial growth factor (VEGF) signaling pathway			hsa04370	VEGF signaling pathway
hsa04510	Focal adhesion			hsa04510	Focal adhesion
hsa01523	Antifolate resistance			hsa01523	Antifolate resistance
hsa04934	Cushing's syndrome			hsa04934	Cushing's syndrome
hsa04213	Longevity regulating pathway - multiple species			hsa04213	Longevity regulating pathway - multiple species
hsa00980	Metabolism of xenobiotics by cytochrome P450			hsa00980	Metabolism of xenobiotics by cytochrome P450
hsa04015	Rap1 signaling pathway			hsa04015	Rap1 signaling pathway
hsa05146	Amoebiasis			hsa05146	Amoebiasis
hsa05120	Epithelial cell signaling in Helicobacter pylori infection			hsa05120	Epithelial cell signaling in Helicobacter pylori infection
hsa04152	AMP-activated protein kinase (AMPK) signaling pathway			hsa04152	AMPK signaling pathway
hsa04217	Necroptosis			hsa04217	Necroptosis
hsa04071	Sphingolipid signaling pathway			hsa04071	Sphingolipid signaling pathway
hsa00910	Nitrogen metabolism			hsa00910	Nitrogen metabolism
hsa04725	Cholinergic synapse			hsa04725	Cholinergic synapse
hsa04658	Th1 and Th2 cell differentiation			hsa04658	Th1 and Th2 cell differentiation
hsa04726	Serotonergic synapse			hsa04726	Serotonergic synapse
hsa00982	Drug metabolism - cytochrome P450			hsa00982	Drug metabolism - cytochrome P450
hsa05144	Malaria			hsa05144	Malaria
hsa04922	Glucagon signaling pathway			hsa04922	Glucagon signaling pathway
hsa04910	Insulin signaling pathway			hsa04910	Insulin signaling pathway
hsa04062	Chemokine signaling pathway			hsa04062	Chemokine signaling pathway
hsa04014	Ras signaling pathway			hsa04014	Ras signaling pathway
hsa01200	Carbon metabolism			hsa01200	Carbon metabolism
hsa04114	Oocyte meiosis			hsa04114	Oocyte meiosis
hsa04728	Dopaminergic synapse			hsa04728	Dopaminergic synapse
hsa05030	Cocaine addiction			hsa05030	Cocaine addiction
hsa04662	B cell receptor signaling pathway			hsa04662	B cell receptor signaling pathway
hsa04976	Bile secretion			hsa04976	Bile secretion
hsa05010	Alzheimer's disease			hsa05010	Alzheimer's disease
hsa04215	Apoptosis - multiple species			hsa04215	Apoptosis - multiple species
hsa04916	Melanogenesis			hsa04916	Melanogenesis
hsa04390	Hippo signaling pathway			hsa04390	Hippo signaling pathway
hsa05020	Prion diseases			hsa05020	Prion diseases
hsa04622	Retinoic acid-inducible gene I (RIG-I)-like receptor signaling pathway			hsa04622	RIG-I-like receptor signaling pathway
hsa01212	Fatty acid metabolism			hsa01212	Fatty acid metabolism
hsa05131	Shigellosis			hsa05131	Shigellosis
hsa05014	Amyotrophic lateral sclerosis (ALS)			hsa05014	Amyotrophic lateral sclerosis (ALS)
hsa00983	Drug metabolism - other enzymes			hsa00983	Drug metabolism - other enzymes
hsa04921	Oxytocin signaling pathway			hsa04921	Oxytocin signaling pathway
hsa04141	Protein processing in endoplasmic reticulum			hsa04141	Protein processing in endoplasmic reticulum
hsa04912	GnRH signaling pathway			hsa04912	GnRH signaling pathway
hsa05231	Choline metabolism in cancer			hsa05231	Choline metabolism in cancer
hsa00071	Fatty acid degradation			hsa00071	Fatty acid degradation
hsa02010	Human ATP-binding cassette (ABC) transporters			hsa02010	ABC transporters
hsa04623	Cytosolic DNA-sensing pathway			hsa04623	Cytosolic DNA-sensing pathway
hsa03320	PPAR signaling pathway			hsa03320	PPAR signaling pathway
hsa05416	Viral myocarditis			hsa05416	Viral myocarditis
hsa05143	African trypanosomiasis			hsa05143	African trypanosomiasis
hsa05016	Huntington's disease			hsa05016	Huntington's disease
hsa00350	Tyrosine metabolism			hsa00350	Tyrosine metabolism
hsa00010	Glycolysis / Gluconeogenesis			hsa00010	Glycolysis / Gluconeogenesis
hsa04540	Gap junction			hsa04540	Gap junction

Table S3 Disease-related genes

Keywords	Related genes
Altitude sickness	*GUCY1A1 SDC4 FOS CA2 CLU TIMP1 CDKN1B JTB KNG2 FAS RAB40C UMOD MPO CYP2B15 CASP3 SMARCC1 STYX ARHGAP45 CA1 CD5 RGS8 CBX3 NKX2-1 CA3 ELANE PLA2G1B RBMX MYO9B NNAT SCHIP1 POU2F1 TRIM25 TMEM30B PTPRR ARHGAP45 CA4 MECR PPM1B BMPR2 ARID2 DDX6 CA12 DDX3X BCKDHB POLR1B SATB1 WNK1 AKAP9 GRK6*
Brain edema	*TNF NOS2 S100B PLAU MYLK MYL9 NAXE ZNHIT3 MMP9 PLAT NTN1 BCL2 CASP3 BAX CAT FOS JUN RELA MAPK3 MAPK1 IL6 CTNNB1 HMOX1 VCAM1 CCL2 IL1B VEGFA GSK3B AGT SOD2 BDNF PTGS2 FAS COL1A1 CREB1 PARP1 NFE2L2 AKT1 CDKN1A NOS3 NFKBIA EGR1 CASP9 MAPK8 SOD1 CCND1 MMP2 BCL2L1 JUNB NFKB1*
Hypoxia, brain	*VEGFA HIF1A NOS2 ITPR2 IRAK1 ITPR1 IRAK4 PNPO HPCAL1 GFAP CDKN1A CCNA2 CASP4 NFKBIA SGK1 NOS1 CTNNB1 CCND1 SLC4A3 MAPK3 MAPK1 CCL2 PLCG1 RGS4 CASP9 TH SPHK1 BCL2L1 MAPK14 GDNF FBXO32 DDIT3 CTSK ADORA1 TP53 NFKBIA MAPK8IP3 TRP53 CREB1 CRH BDNF TRIM63 PLEKHA5 JUN MMP9 RGS2 CREB1 ATF6 CASP8 CYCS*
Hypoxia	*TNF NOS2 S100B PLAU MYLK MYL9 NAXE ZNHIT3 MMP9 PLAT NTN1 BCL2 CASP3 BAX CAT FOS JUN RELA MAPK3 MAPK1 IL6 CTNNB1 HMOX1 VCAM1 CCL2 IL1B VEGFA GSK3B AGT SOD2 BDNF PTGS2 FAS COL1A1 CREB1 PARP1 NFE2L2 AKT1 CDKN1A NOS3 NFKBIA EGR1 CASP9 MAPK8 SOD1 CCND1 MMP2 BCL2L1 JUNB NFKB1*
Hypoxia-ischemia, brain	*VEGFA HIF1A NOS2 IRAK1 IRAK4 PNPO HPCAL1 GFAP CDKN1A CCNA2 CASP4 NFKBIA SGK1 NOS1 CTNNB1 CCND1 MAPK3 MAPK1 CCL2 PLCG1 RGS4 CASP9 TH SPHK1 BCL2L1 MAPK14 GDNF FBXO32 DDIT3 CTSK TP53 MAPK8IP3 TRP53 CRH BDNF TRIM63 PLEKHA5 JUN MMP9 RGS2 CREB1 ATF6 CASP8 CYCS CCND3 SQSTM1 CASP3 VCAM1 ARHGAP29 GSK3B*
Polycythemia	*GH1 JAK2 EPOR BPGM EGLN1 EPAS1 EPOR HBA1 HBB JAK2 SH2B3 SLC30A10 VHL GSK3B ENG BAX PPARGC1A EDNRA EDN1 CYBA IL1B IL1A NOS3 TYK2 ITPKB COL1A1 KCND3 IL6 CD151 PPIB ACE COL3A1 SIVA1 PRKCA TOMM20 NFE2L1 RELA PDE10A PRL XDH AGTR2 BCL2 ATRX TLR4 TGFB1 CYP19A1 CKS2 FOS CREB1 CYCS*
Pulmonary arterial hypertension	*BMPR2 CTNNB1 AGTR1 APECAM1 ACE2 EDNRA MYD88 VEGFA NOX4 TNFRSF13C BCL2A1B ACE GFAP TFRC MS4A6D CLEC5A CRLF2 GPR65 NOS2 TNFSF10 IL18 RELA TREM1 CD19 CXCL10 CLEC4E MS4A1 KCNE2 CCL5 TLR4 FNDC1 CAR8 CXCL1 LYVE1 IL17RA NOD2 RETNLA CD3G RMDN2 TIMP1 CD22 VCAM1 EDN1 GSK3B POLR1B MAPK3 MAPK1 IRAK3 TLR9 KCNB1*
Pulmonary edema of mountaineers	*GUCY1A1 SMARCC1 ARHGAP45 CBX3 RBMX POU2F1 TRIM25 CA1 PPM1B BMPR2 CA12 DDX3X AKAP9 ANP32A ITPR2 CA9 CD47 CIRBP HTRA1 SC5D AQP1 CA2 NDRG1 CCND2 MT1 EDN1 FOS BEC-1 CA6 FAM192BP ZFP617 CA7 CA14 AKAP17B ZFP322A CA5B ADA2B CA15A CBLN6 CCL19A.2 CTAGE3P EPA1 FGFBP2A H41 HCCSB LRRC2-AS1 MRPS31P5 RCP9 RHOXF2B SAS10*

https://dx.doi.org/10.21037/atm-22-2111